decrease of the platinum–oxygen bond lengths from 2.829 (5) to 2.221 (9) Å it can be seen in Figure 4 that the naphthyl ligand in **7** is pivoted about an axis through carbon, C(201), normal to the ligand plane, such as to move the methoxy oxygen somewhat away from the platinum, presumably to minimize nonbonding repulsions. This is reflected by the inequivalent bond angles about the carbon bonded to platinum. With the coordination of this oxygen in compound **15**, the naphthyl ligand appears to pivot about the Pt-bonded carbon atom, C(101), again but this time in the opposite sense to bring the oxygen of the methoxy group much closer to the platinum, and the bond angles about this carbon atom are now reversed from those in **7**.

Only a few other structurally characterized cis addition products have previously been reported. Reaction of $[Pt\{2\text{-}C_6H_4N(O)O\}_2]$ with MeI and halogens afforded $[Pt\{2\text{-}C_6H_4N(O)O\}_2Me(I)]$ and $[Pt\{2\text{-}C_6H_4N(O)O\}_2X_2]$ (X = Cl, Br, I), respectively, which were characterized by ^1H NMR spectroscopy.[46] Interestingly these complexes also contain oxygen donor atoms in the cyclometalating ring, pointing to an important influence of the nature of the donor atom on the stereochemistry of the formed products. A photochemically induced cis oxidative addition was observed in the reaction of MeI, CH_2Cl_2, or (*E*)-ClCH=CHCl with *cis*-bis(2-phenylpyridine)platinum(II) and *cis*-bis{2-(2-thienyl)pyridine}-platinum(II), respectively.[47] On the basis of their ^1H NMR spectra, it was concluded that all these complexes were formed in only one isomeric form.

Acknowledgment. The Commission of the European Communities (Contract No. ST2J-0090-1-F(CD)) is thanked for its financial support. This work was also supported (A.L.S.) by the Netherlands Foundation for Chemical Research (SON) with financial aid from the Netherlands Organization for the Advancement of Pure Research (ZWO). We thank A. J. M. Duisenberg for collecting the diffraction data and Prof. K. Vrieze and Dr. D. M. Grove for their interest in this research.

Registry No. **1**, 86526-70-7; **2**, 51179-24-9; **3**, 116840-82-5; **4**, 116840-83-6; **5**, 116840-84-7; **6**, 116840-85-8; **7**, 87370-33-0; **8**, 116840-86-9; **9**, 116840-87-0; **10**, 116840-88-1; **11**, 116840-89-2; **12**, 116840-90-5; **13**, 116840-91-6; **14**, 116840-92-7; **15**, 116840-93-8; **16**, 116840-94-9; $[PtCl_2(COD)]$, 12080-32-9; $[PtCl_2(Et_2S)_2]$, 14873-92-8; [Li(DMBA)], 60528-57-6; *cis*-bis(8-methoxynaphthyl)platinum diiodide, 116908-91-9.

Supplementary Material Available: A full table of crystallographic data, listings of thermal parameters, hydrogen atom positions, thermal parameters, and all bond distances and bond angles for **6** and **7**, listings of disordered solvate positions, thermal parameters, hydrogen atom positions, and all bond distances and angles for **15**, and ORTEP projections for **6**, **7**, and **15** (21 pages); listings of observed and calculated structure factors (102 pages). Ordering information is given on any current masthead page.

(45) We thank one of the reviewers for drawing our attention to these interesting structural differences in the various MXN moieties.
(46) Vicente, J.; Chicote, M. T.; Martin, J.; Jones, P. G.; Fittschen, C. *J. Chem. Soc., Dalton Trans.* **1987**, 881.
(47) (a) Chassot, L.; von Zelewsky, A. *Helv. Chim. Acta* **1986**, *69*, 1855. (b) Chassot, L.; von Zelewsky, A.; Sandrini, D.; Maestri, M.; Balzani, V. *J. Am. Chem. Soc.* **1986**, *108*, 6084.

Contribution from the Department of Chemistry, University of California, Irvine, California 92717

Synthetic and Structural Studies on the Formation of a Tetradecametallic Yttrium Oxide Alkoxide Chloride Complex: An Example of How Molecular Yttrium Oxygen Frameworks Form Extended Arrays[1]

William J. Evans* and Mark S. Sollberger

Received July 29, 1988

YCl_3 reacts with 2 equiv of $NaOCMe_3$ in THF to form $Y_3(OCMe_3)_7Cl_2(THF)_2$ (**1**) in 80% yield. The yttrium atoms in this molecule form a triangle that has doubly bridging alkoxide groups along each edge, a μ_3-$OCMe_3$ group on one side of the Y_3 plane, and a μ_3-Cl ligand on the other side. One metal is coordinated to a terminal chloride ion and a terminal alkoxide group. Each of the other metals is coordinated to a terminal alkoxide group and a molecule of THF. Both chloride ions lie on the same side of the Y_3 plane as the two THF ligands. In toluene under nitrogen over a period of 2 weeks, **1** converts to $Y_{14}(OCMe_3)_{28}Cl_{10}O_2(THF)_4$ (**2**) in quantitative yield. **2** is comprised of four trimetallic $Y_3(\mu_3\text{-}OR)(\mu_3\text{-}X)(\mu\text{-}Z)_3$ units (where X = Cl, O; Z = Cl, $OCMe_3$) that have structures similar to the $Y_3(\mu_3\text{-}OR)(\mu_3\text{-}Cl)(\mu\text{-}OR)_3(OR)_3Cl(THF)_2$ structure of **1**. The four trimetallic subunits in **2** are connected by two μ-Cl ions, a μ_4-O ion and a $[(\mu\text{-}OR)_2Y(\mu\text{-}Cl)]_2$ group. Complex **2** is a dimer, $\{[Y_3(\mu_3\text{-}OR)(\mu_3\text{-}Cl)(\mu\text{-}OR)_3(OR)_3(THF)_2](\mu\text{-}Cl)[Y_3(\mu_3\text{-}OR)(\mu\text{-}OR)_2(\mu\text{-}Cl)(OR)_2](\mu_4\text{-}O)[(\mu\text{-}OR)_2Y(\mu\text{-}Cl)]\}_2$, which contains a center of inversion. **1** crystallizes from THF in the space group $P2_1/c$ with unit cell dimensions a = 18.102 (7) Å, b = 15.871 (6) Å, c = 21.084 (5) Å, β = 104.87 (3)° and Z = 4 for D_{calcd} = 1.291 g cm^{-3}. Least-squares refinement on the basis of 2435 observed reflections led to a final R value of 0.136. **2** crystallizes from toluene in the space group $P\bar{1}$ with unit cell dimensions a = 17.373 (14) Å, b = 18.343 (11) Å, c = 19.278 (10) Å, α = 99.75 (5)°, β = 92.26 (6)°, γ = 114.15 (5)° for Z = 2 and D_{calcd} = 1.313 g cm^{-3}. Least-squares refinement on the basis of 3830 observed reflections led to a final R value of 0.114.

Introduction

The conversion of alkoxide compounds to oxides via sol–gel processes has been studied extensively as a route to high-purity oxides and thin-film coatings.[2-11] Much of this research has centered on silicon alkoxides, although some transition-metal systems have also been studied.[9-18] The transition-metal systems

(1) Reported in part at the 2nd International Conference on the Basic and Applied Chemistry of f-Transition (Lanthanide and Actinide) and Related Elements, Lisbon, Portugal, April 1987; paper L(II)1.
(2) *Better Ceramics Through Chemistry*; Brinker, C. J., Clark, D. E., Ulrich, D. R., Eds.; Materials Research Society Symposia Proceedings 32; Elsevier: New York, 1984.
(3) *Better Ceramics Through Chemistry II*; Materials Research Society Symposia Proceedings 73; Elsevier: New York, 1986.
(4) Dislich, H. *J. Non-Cryst. Solids* **1985**, *73*, 599–612.
(5) Roy, R. *J. Am. Ceram. Soc.* **1969**, *52*, 344.
(6) Yoldas, B. E. *Am. Ceram. Soc. Bull.* **1980**, *59*, 479–483.
(7) Klein, L. C. *Ann. Rev. Mater. Sci.* **1985**, *15*, 227–248.
(8) Hench, L. L., Ulrich, D. R., Eds. *Ultrastructure Processing of Ceramics, Glasses and Composites*; Wiley: New York, 1984, and references therein.
(9) Hubert-Pfalzgraf, L. G. *New J. Chem.* **1987**, *11*, 663–675.
(10) Zelinski, B. J.; Uhlmann, D. R. *J. Phys. Chem. Solids* **1984**, *45*, 1069–1090.
(11) Dislich, H. *Angew. Chem., Int. Ed. Engl.* **1971**, *10*, 363–369.

0020-1669/88/1327-4417$01.50/0

Table I. NMR Data for Complexes **1–3**

		^{1}H NMR,[a,b] δ		
complex	solvent	μ_3-$OCMe_3$	μ-$OCMe_3$	$OCMe_3$
1	THF-d_8[b]	1.90 (s,9 H)	1.51 (s, 18 H) 1.45 (s, 9 H)	1.32 (s, 18 H), 1.26 (s, 9 H)
2	THF-d_8[b]	1.90 (s, 18 H) 1.65 (s, 18 H)	1.51 (s, 108 H) 1.45 (s, 18 H)	1.32 (s, 36 H), 1.26 (s, 54 H)
3	THF-d_8[b]	1.88 (s, 9 H)	1.50 (s, 18 H) 1.43 (s, 9 H)	1.31 (s, 18 H), 1.24 (s, 9 H) 1.22 (s, 9 H)

		^{13}C NMR,[a] δ		
complex	solvent	$OCMe_3$	$OC(CH_3)_3$	THF
1	THF-d_8	77.70, 74.61, 73.70 73.39, 73.08	36.49, 36.15, 36.08 35.68, 35.33	69.42 27.58

[a] Referenced to residual H at δ 1.79 and C_α at δ 68.6 [b] Coordinated THF is seen as a broad singlet at approximately 0.45 ppm upfield from the solvent peaks.

of particular interest are those that form electroceramics, e.g., barium titanate,[12,16,17] and thin films with special physical properties.[19-23]

Although many investigations of the conversion of alkoxides to oxide materials have been conducted, the complexity of these systems[2-8] has made it difficult to clearly establish the details of these processes at the molecular level. Structural connections between molecular metal alkoxides and metal oxides are well established,[24-29] but less is known about alkoxide to oxide transformations. General schemes can be written for the hydrolysis of metal alkoxides, $M(OR)_x$, followed by condensation of resulting MOH units to form M–O–M linkages,[9-11] but specific molecular examples are rare.[24] The structures of a few highly condensed early-transition-metal alkoxide complexes isolated from hydrolysis reactions have been reported,[25-27] but the connection of these structures to the hydrolysis chemistry of their precursors is not clear.

We report here the conversion of a trimetallic yttrium alkoxide complex to a tetradecametallic yttrium alkoxide oxide complex, which constitutes a well-defined example of how a molecular complex begins to form an extended polymetallic material. These results suggest that molecular metal alkoxide chemistry may provide useful information related to the conversion of polymetallic alkoxides to polymetallic oxides.

(12) Mazdiyasni, K. S.; Dolloff, R. T.; Smith, J. S. *J. Am. Ceram. Soc.* **1969**, *52*, 523–526.
(13) Smith, J. S.; Dolloff, R. T.; Mazdiyasni, K. S. *J. Am. Ceram. Soc.* **1970**, *53*, 91–95.
(14) Riman, R. E.; Haaland, D. M.; Northrup, C. J. M.; Bowen, H. K.; Bleier, A. *Mater. Res. Soc. Symp. Proc.* **1984**, *32*, 233–238.
(15) Ayen, R. J.; Burk, J. H. *Mater. Res. Soc. Symp. Proc.* **1986**, *73*, 801–808.
(16) Ritter, J. J.; Roth, R. S.; Blendell, J. E. *J. Am. Ceram. Soc.* **1986**, *69*, 155–161.
(17) Phule, P. P.; Raghavan, S.; Risbud, S. H. *J. Am. Ceram. Soc.* **1987**, *70*, C108–C109.
(18) Fegley, B., Jr.; White, P.; Bowen, H. K. *Am. Ceram. Soc. Bull.* **1985**, *64*, 1115–1120.
(19) Livage, J. *Mater. Res. Soc. Symp. Proc.* **1984**, *32*, 125–134.
(20) Sakka, S.; Kamiya, K.; Makita, K.; Yamamoto, Y. *J. Non-Cryst. Solids* **1984**, *63*, 223–235.
(21) Dosch, R. G. *Mater. Res. Soc. Symp. Proc.* **1984**, *32*, 157–161.
(22) Chen, K. C.; Janah, A.; Mackenzie, J. D. *Mater. Res. Soc. Symp. Proc.* **1986**, *73*, 731–736.
(23) Silverman, L. A.; Teowee, G.; Uhlmann, D. R. *Mater. Res. Soc. Symp. Proc.* **1986**, *73*, 725–730.
(24) Bradley, D. C.; Mehrotra, R. C.; Gauer, D. P. *Metal Alkoxides*; Academic: New York, 1978.
(25) Watenpaugh, K.; Caughlan, C. N. *Chem. Commun.* **1967**, 76–77.
(26) Bradley, D. C.; Hursthouse, M. B.; Rodesiler, P. F. *Chem. Commun.* **1968**, 1112–1113.
(27) Morosin, B. *Acta Crystallogr., Sect. B* **1977**, *B33*, 303–305.
(28) Chisholm, M. H. *J. Solid State Chem.* **1985**, *57*, 120–133 and references therein.
(29) Chisholm, M. H.; Hampden-Smith, M. *J. Am. Chem. Soc.* **1987**, *109*, 5871–5872 and references therein.

Table II. Crystallographic Data for **1** and **2**

	1	**2**
formula	$Y_3C_{36}H_{79}O_9Cl_2(C_4H_8O)_2$	$Y_7C_{64}H_{142}O_{17}Cl_5(C_7H_8)_2$
mol wt	1137.85	2167.70
space group	$P2_1/c$	$P\bar{1}$
cell const		
a, Å	18.102 (7)	17.373 (14)
b, Å	15.871 (6)	18.343 (11)
c, Å	21.084 (5)	19.278 (10)
α, deg		99.75 (5)
β, deg	104.87 (3)	92.26 (6)
γ, deg		114.15 (5)
cell vol, Å^3	5854 (3)	5484 (6)
molecules/unit cell	4	2
D_{calcd}, g cm^{-3}	1.291	1.313
temp, K	298	298
μ_{calcd}, cm^{-1}	31.01	38.55
radiation	Mo Kα; λ = 0.71073 Å	Mo Kα; λ = 0.71073 Å

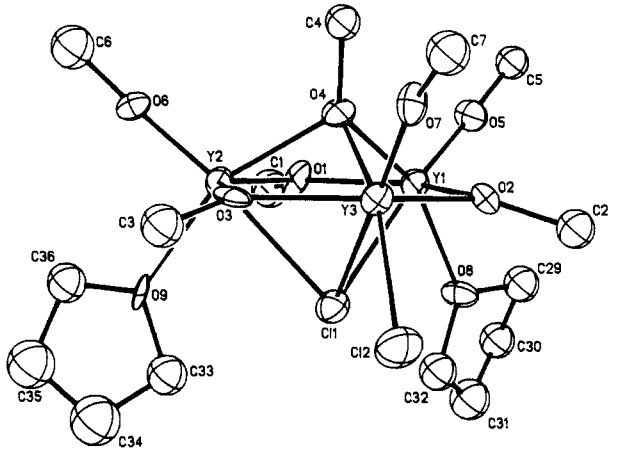

Figure 1. Molecular structure of $Y_3(\mu_3\text{-}OR)(\mu_3\text{-}Cl)(\mu\text{-}OR)_3(OR)_3Cl(THF)_2$ (**1**) (R = *tert*-butyl). For clarity, 20% probability ellipsoids have been used and the methyl groups of the *tert*-butoxide ligands are omitted.

Results

A summary of the chemistry presented in this section is given in Scheme I.

Scheme I

$$YCl_3 + 2NaOCMe_3 \xrightarrow{THF} \underset{\mathbf{1},\ 80\%}{Y_3(OCMe_3)_7Cl_2(THF)_2} \quad (1)$$

$$\underset{\mathbf{1}}{Y_3(OCMe_3)_7Cl_2(THF)_2} \xrightarrow{toluene} \underset{\mathbf{2},\ \text{quantitative}}{[Y_7(OCMe_3)_{14}Cl_5O(THF)_2]_2} \quad (2)$$

$Y_3(\mu_3\text{-}OCMe_3)(\mu_3\text{-}Cl)(\mu\text{-}OCMe_3)_3(OCMe_3)_3Cl(THF)_2$ (1). The reaction of YCl_3 with 2 equiv of $NaOCMe_3$ in THF gives

Table III. Selected Bond Length Ranges (Å) in Complexes 1–4

		$[Y_7Cl_5(OR)_{14}(THF)_2O]_2$ (2)				
	$Y_3Cl_2(OR)_7(THF)_2$ (1)	unit A	unit B	unit C	$Y_3Cl(OR)_8(THF)_2$ (3)	$Y_4Cl_2(OR)_{10}O$ (4)
Y–O(OR)	1.97 (2)–2.01 (2)	2.01 (3)–2.07 (3)	2.03 (4)–2.06 (3)		2.037 (11)–2.073 (15)	2.02 (2)–2.07 (2)
Y–O(μ-OR)	2.25 (2)–2.32 (2)	2.24 (3)–2.34 (3)	2.21 (3)–2.30 (3)	2.22 (3)–2.29 (3)	2.241 (10)–2.358 (10)	2.26 (2)–2.34 (2)
Y–O(μ_3-OR)	2.36 (2)–2.45 (3)	2.35 (2)–2.40 (3)	2.39 (3)–2.47 (3)		2.306 (8)–2.556 (13)	2.35 (2)–2.44 (2)
Y–O(μ_4–O)			2.13 (2)–2.37 (2)	2.13 (2)		2.40 (2)–2.52 (2)
Y–O(THF)	2.36 (2)–2.45 (2)	2.33 (4)–2.37 (3)			2.417 (12)	
Y–Cl	2.595 (12)					
Y–Cl(μ–Cl)		2.730 (12)	2.709 (11)–2.754 (12)	2.723 (11)–2.820 (11)		2.681 (9)–2.700 (8)
Y–Cl(μ_3–Cl)	2.831 (10)–2.885 (10)	2.825 (13)–2.856 (12)			2.820 (5)–2.897 (6)	
Y···Y	3.52–3.78	3.55	3.34–3.54	3.57–3.60	3.50–3.63	3.46–3.62

a single primary product, **1**, in 80% yield (eq 1). The ^{1}H NMR spectrum of **1** in THF-d_8 consisted of five peaks in the alkoxide region at δ 1.90–1.26 with an integrated ratio of 1:2:1:2:1. This spectrum was similar to the ^{1}H NMR spectrum for the crystallographically characterized complex $Y_3(\mu_3\text{-}OCMe_3)(\mu_3\text{-}Cl)(\mu\text{-}OCMe_3)_3(OCMe_3)_4(THF)_2$ (**3**),[30] which contains six peaks in a 1:2:1:2:1:1 ratio (Table I). We previously have noted a correlation between chemical shift and coordination mode of the alkoxide groups in molecules of this type:[30,31] terminal alkoxides are found at highest field, doubly bridging alkoxides are found at lower field, and triply bridging groups are observed furthest downfield. The chemical shifts of the five lowest field resonances for **1** and **3** are within 0.02 ppm of each other. Only the δ 1.22 resonance in **3**, attributed to a terminal alkoxide group, is missing in **1**. Thus, if one uses the structure/shift correlations established for **3**, the ^{1}H NMR spectrum of **1** corresponded to one triply bridging alkoxide group, two types of doubly bridging groups in a ratio of 2:1, and two types of terminal alkoxide groups in a ratio of 2:1. This is exactly what was found by X-ray crystallography (see below).

The ^{13}C NMR spectrum of **1** is consistent with the ^{1}H NMR data. Five quaternary carbon resonances are found in the δ 78–72 range, one for each of the five chemically distinct alkoxide groups, and five methyl signals are found in the δ 37–35 range. These values fall within the chemical shift ranges previously observed for **3**. Like **3**, the NMR spectrum of **1** in aromatic solvents showed fluxional behavior for the alkoxide groups. The IR spectrum for **1** is indistinguishable from that of **3**.

X-ray crystallography (Table II) showed that complex **1** (Figure 1) is structurally similar to **3** except that one terminal alkoxide group in **3** has been replaced by a terminal chloride ligand. The trimetallic **1** has a trigonal-planar arrangement of the yttrium atoms, doubly bridging alkoxide groups along the edges of the Y_3 triangle, and triply bridging groups above and below the Y_3 plane, a μ_3-$OCMe_3$ group and a μ_3-Cl ligand, respectively. Two of the yttrium atoms, Y(1) and Y(2), each have a terminal alkoxide ligand and are ligated by a molecule of THF; the third yttrium atom is coordinated by a chloride ion and an alkoxide group. Thus, each yttrium atom in **1** is six-coordinate.

The gross geometry of **1** is well established from the X-ray data and is consistent with the spectroscopic and analytical data. However, as a result of the rather significant crystal decay during data collection, the bond length and angle data can only be evaluated approximately in terms of averages (Table III).

The structure of **1** displays features very similar to those found in **3**[30] and the tetrametallic species $[Y_4(\mu_3\text{-}OCMe_3)_2(\mu\text{-}OCMe_3)_4(OCMe_3)_4(\mu\text{-}Cl)_2(\mu_4\text{-}O)Li_4(\mu\text{-}OCMe_3)_2]_2$ (**4**),[30] whose core structure is shown schematically in Figure 2. As shown in Table III, the Y–OR distances of **1** fall within the range of values previously observed for complexes of this type. The terminal alkoxide groups have the shortest distances, doubly bridging groups have longer Y–OR bonds, and triply bridging alkoxides have the longest Y–O bond lengths. The Y–O(THF) bond distances and

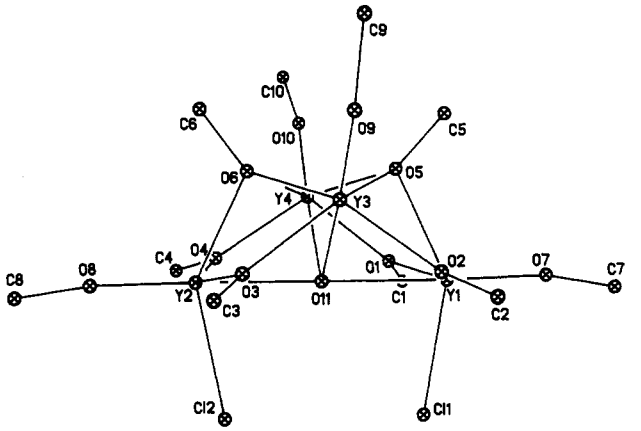

Figure 2. Configuration of the $Y_4(\mu_3\text{-}OR)_2(\mu\text{-}OR)_4(OR)_4Cl_2^{2-}$ unit in **4** (R = *tert*-butyl).[30]

Y–Cl distances in **1** are also similar to those in **3** and **4**.

Complex **1** is also similar to **3** in that it contains variations in structural features that suggest the molecule is sterically congested. In **3**, the bond distances to the $Y(OR)_2$ unit were greater than those to the Y(OR)(THF) counterparts. In **1**, the Y(OR)Cl unit (Y(3)) has the longer distances compared to the Y(OR)(THF) units (Y(1) and Y(2)). In addition, the Y(3)–O(7)–C(7) angle associated with the Y(OR)Cl unit is bent to 163.3 (26)°, which moves the *tert*-butyl group away from the more sterically congested center of the molecule. The other terminal Y–O–CR_3 bonds are nearly linear with an average angle of 175.4°. Also as in **3**, the oxygen atoms of the μ-OR groups are displaced from the Y_3 plane in the direction of the μ_3-Cl ligand: 0.058 Å for O(1), 0.061 Å for O(2), and 0.056 Å for O(3).

$[Y_7(\mu_3\text{-}OCMe_3)_2(\mu_3\text{-}Cl)(\mu_4\text{-}O)(\mu\text{-}OCMe_3)_7(OCMe_3)_5(\mu\text{-}Cl)_4(THF)_2]_2$ (2). When complex **1** is left in toluene for a period of 2 weeks, it converts to **2** (eq 2). The ^{1}H NMR spectrum of **2** differed significantly from that of **1** or **3** and had a total of six peaks in a ratio of 1:1:6:1:2:3 in the δ 1.90–1.26 region. Two of these peaks, δ 1.90 and 1.65, are in the region normally associated with μ_3-$OCMe_3$ groups. The complexity of the NMR spectrum of **2** indicated that a more complicated structure was present. Indeed this was the case. The structure of **2**, determined by X-ray crystallography, is shown in Figure 3. A summary of bond distances is given in Table III.

Since complex **2** contains an inversion center, only seven of the 14 yttrium atoms are crystallographically independent. For discussion, the crystallographically unique half of **2** will be divided into two trimetallic fragments, A and B, and half of a bimetallic $[(RO)_2YCl]_2$ fragment, C. To illustrate the relationship of complex **2** to complexes **1**, **3**, and **4** more clearly, we will define formulas for A–C that do not describe the bridging *between* the fragments. Therefore, we will define A as $[Y_3(\mu_3\text{-}OR)(\mu_3\text{-}Cl)(\mu\text{-}OR)_3(OR)_3Cl(THF)_2]$, B as $[Y_3(\mu_3\text{-}OR)(\mu_3\text{-}O)(\mu\text{-}OR)_2(\mu\text{-}Cl)(OR)_2Cl]$, and C as $[(RO)_2YCl]$ (see Figure 3).

The formula unit for A is the same as that for **1**, $Y_3(\mu_3\text{-}OR)(\mu_3\text{-}Cl)(\mu\text{-}OR)_3(OR)_3Cl(THF)_2$, and structurally, these units are nearly identical. As shown in Table III, the terminal alkoxide distances, the bridging Y–O(μ-OR) and Y–O(μ_3-OR) distances,

(30) Evans, W. J.; Sollberger, M. S.; Hanusa, T. P. *J. Am. Chem. Soc.* **1988**, *110*, 1841–1850.
(31) Brown, L. M.; Mazdiyasni, K. S. *Inorg. Chem.* **1970**, *9*, 2783–2786.

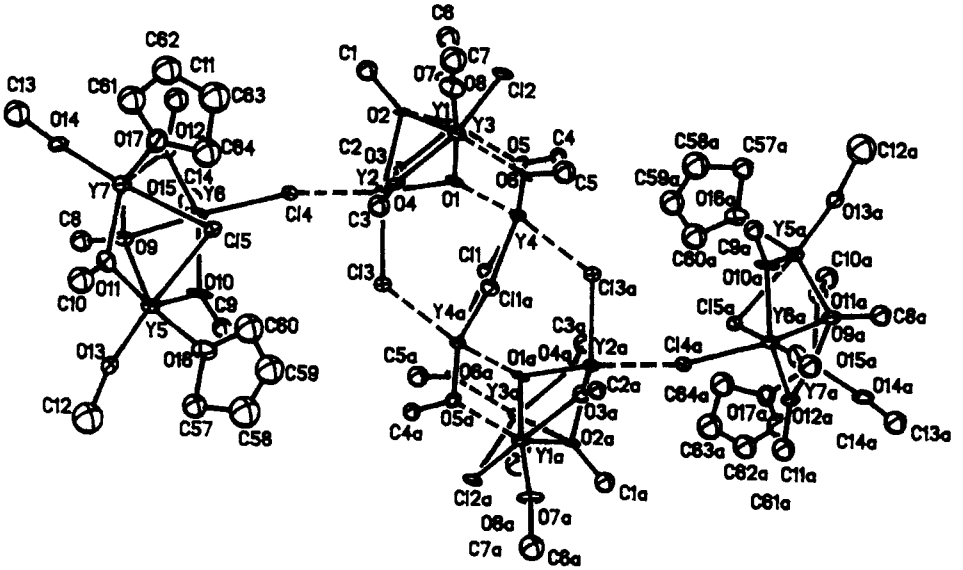

Figure 3. Molecular structure of $[Y_7(\mu_3\text{-OR})_2(\mu_3\text{-Cl})(\mu_4\text{-O})(\mu\text{-OR})_7(OR)_5(\mu\text{-Cl})_4(THF)_2]_2$ (**2**) (R = *tert*-butyl). For clarity, 20% probability ellipsoids have been used and the methyl groups of the *tert*-butoxide ligands omitted. For the purposes of the discussion, this structure has been divided into three parts. Dashed line bonds have been put in to show the separation of these units: A, Y(5)–Y(7); B, Y(1)–Y(3); C, Y(4).

the Y-Cl(μ_3-Cl) distances, and the Y–O(THF) distances are similar to those in **1**, **3**, and **4**. The main bond length difference between **1** and A involves the remaining chloride ligand. The Y–Cl distance in A, 2.730 (12) Å, is significantly longer than the terminal Y–Cl distance in **1**, 2.595 (12) Å. However, this is not unexpected since this chloride in A is the bridging atom that connects A to B. This Y–Cl distance in A is close to the Y–Cl(μ-Cl) distances in **4** (2.681 (9)–2.700 (8) Å).

The A part of complex **2** is also similar to **1** and **3** in that there are some slight distortions in the structure that may be due to steric crowding. There are no significant differences in the bond distances to the Y(OR)Cl unit of A, Y(6), compared to the Y(5) and Y(7) counterparts. However, the triply bridging ligands are distorted such that the μ_3-OR group is pushed closer to Y(5) and the μ_3-Cl ligand is closer to Y(6) and Y(7). In addition, O(10), O(11), and O(12) are displaced from the Y_3 plane in the direction of the μ_3-chloride by 0.062, 0.112, and 0.024 Å, respectively. These variations again are likely to occur in order to best accommodate steric congestion.

The trimetallic B part of **2**, which contains Y(1), Y(2), and Y(3), is also similar to **1**, although it is not as similar to **1** as A because it has a slightly different ligand set. B contains an oxide ion in place of the μ_3-Cl ligand in **1**, and a bridging chloride ion has replaced a μ-OR ligand. To compensate for the charge difference caused by replacing a Cl^- ion by an O^{2-} ion, only three terminal anionic ligands are associated with B, in contrast to the four present in **1**. In addition to these differences, one of the positions occupied by a terminal alkoxide ligand in **1** is now occupied by a chloride ion in B. This chloride ion in B forms a bridge to C. The positions occupied by terminal THF ligands in **1** are occupied in B by bridging alkoxide groups that are also associated with unit C.

The Y–OR and Y–Cl bond distances in B fall within the range of values observed for **1**, A, **3**, and **4** (Table III). The yttrium–oxide distances in B, Y(2)–O(1) = 2.13 (2) Å, Y(1)–O(1) = 2.37 (2) Å, and Y(3)–O(1) = 2.32 (2) Å, are much shorter than the Y–O(oxide) distances in **4**, Y–O(oxide) = 2.40 (2)–2.52 (2) Å. They are more comparable to the range found for yttrium oxide distances in $(C_5H_5)_5Y_5(\mu\text{-}OCH_3)_4(\mu_3\text{-}OCH_3)_4(\mu_5\text{-O})$ (**5**),[32] 2.27 (2)–2.41 (2) Å. However, the Y(2)–O(1) distance is still shorter than this range and is even shorter than the Y–O distance in Y_2O_3 of 2.28 Å.[33]

In **1**, **3**, and A the interaction of three terminal alkoxide groups with a μ_3-OR group resulted in steric congestion and structural distortion. In B there are only two terminal alkoxide groups, and hence there is less crowding around the μ_3-OR ligand. In fact in B, the doubly bridging ligands are displaced out of the Y_3 plane *toward* the μ_3-OR ligand: 0.054, 0.113, and 0.304 Å for O(3), O(4), and Cl(2), respectively.

The presence of only three terminal anionic ligands and the absence of any neutral THF ligands in the fragment defined as B leaves each metal coordinatively unsaturated. These coordinative vacancies are filled by linking B to A and C via bridging ligands. Fragment A links to B through a chloride ligand on A, Cl(4), with a normal Y(2)–Cl(μ-Cl) distance of 2.754 (12) Å. The $(RO)_2YCl$ fragment, C, links to B through its two alkoxide ligands with a 2.30 (3) Å Y(1)–O(5) and a 2.29 (3) Å Y(3)–O(6) connection.

What remains to be described in the structure of **2** is the $(RO)_2YCl$ fragment C. The yttrium atom in C is six-coordinate as are all of the other yttrium atoms in **2**. Three positions are occupied by the two alkoxides and the chloride ion in the formula unit. The other coordination positions are filled by the oxide ion in B, a chloride ion in the other B fragment (i.e., B′ related to B by the inversion center), and a chloride ion from the other C fragment (i.e., C′). Since the alkoxide ligands in the formula unit for C bridge to B and the chloride in the formula unit for C bridges to C′, all six ligands around the yttrium atom in C are bridging.

Five of the six Y(4)–ligand distances in C are in the normal range (Table III). On the other hand, the Y(4)–Cl(3a) connection between C and B′, 2.820 (11) Å, is long for a Y–Cl(μ-Cl) distance. The longest previously reported distance of this type was the 2.776 (5) Å length in $(C_5Me_5)_2Y(\mu\text{-Cl})YCl(C_5Me_5)_2$.[34] The Y(4)–Cl(3a) distance is comparable to the Y–Cl(μ_3-Cl) lengths in **1**–**4**.

Looking at fragments B and C together, i.e., the four yttrium atoms, Y(1)–Y(4), we can make an interesting comparison with the tetrametallic complex **4**. Complex **4** (Figure 2) was previously described as two trimetallic units fused together along one edge.[30] The structure contained a butterfly arrangement of four metals with a rigorously linear Y–O–Y angle involving the wing tip yttrium atoms and the central μ_4-oxide, Y(1)–O(11)–Y(2), and approximately 90° Y–O–Y bond angles involving Y(3) and Y(4), i.e., [Y(1) or Y(2)]–O(11)–[Y(3) or Y(4)]. In **2**, the arrangement of Y(1)–Y(4) around the μ_4-oxide is more nearly tetrahedral with an average Y–O(1)–Y bond angle of 108.1°. As a result, Y(4) is too far away from Y(3) and Y(1) to interact with a triply bridging ligand in a structure analogous to that of **4**. If Y(4)

(32) Evans, W. J.; Sollberger, M. S. *J. Am. Chem. Soc.* **1986**, *108*, 6095–6096.
(33) O'Connor, G. H.; Valentine, T. M. *Acta Crystallogr., Sect. B* **1969**, *B25*, 2140–2144.
(34) Evans, W. J.; Peterson, T. T.; Rausch, M. D.; Hunter, W. E.; Zhang, H.; Atwood, J. L. *Organometallics* **1985**, *4*, 554–559.

moved closer to Y(1) and Y(3) such that the Y(4)–O(1)–Y(2) angle were nearly linear, Cl(2) could triply bridge Y(1), Y(3), and Y(4). If Cl(3a) were a terminal ligand and if the Y(4)–Cl(1a) interaction did not exist, the structure would be analogous to that of **4**. Hence, B and C taken together constitute another structural variation of a four-yttrium unit.

A retrospective look at the ^{1}H NMR spectrum of **2** shows that five of the six peaks observed for **2** coincide exactly with those for **1**. This correlates with unit A above. Subtracting out the area due to A from the NMR resonances of **2** leaves the six resonances with a 0:1:4:0:0:2 intensity ratio. Again, if one uses the structure/shift correlations established for **1** and **3**, this corresponds to one new μ_3-OR group, four new μ-OR groups, and two new terminal OR groups. The μ_3-OR ligand along with the two terminal OR groups and two of the four μ-OR ligands correlates with unit B. The remaining two μ-OR ligands then correlate with unit C. The different types of terminal ligands and μ-OR bridging ligands in A, B, and C are not resolved in the spectrum. This is not unreasonable since they are placed in very similar chemical environments. We were fortunate in being able to make the rather detailed correlation between the structure and NMR spectrum of **2** since it rearranges in THF over a period of 24 h to form **1** and some as yet undetermined products. As was the case with complexes **1** and **3**, the NMR spectrum of **2** in aromatic solvents shows fluxional behavior for the alkoxide groups.

Scheme II. Reactions of YCl_3 with Alkali-Metal *tert*-Butoxide Reagents (R = CMe_3)

$$YCl_3 + 3NaOR \rightarrow \underset{\mathbf{3},\ 80\%}{Y_3(OR)_8Cl(THF)_2} \quad (3)$$

$$YCl_3 + 3LiOR \rightarrow \text{complex mixture} \quad (4)$$

$$YCl_3 + 2NaOR \rightarrow \underset{\mathbf{1},\ 80\%}{Y_3(OR)_7Cl_2(THF)_2} \quad (5)$$

$$YCl_3 + 2LiOR \rightarrow \text{complex mixture that includes } \{[Y_4(OR)_{10}Cl_2O][Li_4(OR)_2]\}_2 \quad (6)$$

Discussion

Synthesis. Scheme II summarizes how YCl_3 reacts with 2 and 3 equivalents of sodium and lithium *tert*-butoxide (R = CMe_3). The synthetic chemistry of the yttrium *tert*-butoxide system is clearly more complicated than indicated by the earlier literature on YCl_3/NaOR reactions in which simple $[Y(OR)_3]_n$ product formulas are cited.[24,31,35,36] Reactions 3 and 5 are also more complicated than their cyclopentadienyl counterparts, reactions 7[37] and 8.[38] In the cyclopentadienyl systems, for a given reaction

$$YCl_3 + 3NaC_5H_5 \xrightarrow{THF} (C_5H_5)_3Y(THF) + 3NaCl \quad (7)$$

$$YCl_3 + 2NaC_5H_5 \xrightarrow{THF} (C_5H_5)_2YCl(THF) + 2NaCl \quad (8)$$

stoichiometry, there is generally only one type of available product. In contrast, given the geometry and polymetallic nature of trimers **1** and **3**, several isomers are possible. Hence, with yttrium and, more generally, the lanthanide elements,[30] the *tert*-butoxide group will not be a simple equivalent of the cyclopentadienyl ligand.

However, despite these apparent complications, the synthetic chemistry of trimetallic **1** and **3** appears quite manageable. For example, each complex is obtained in high yield and as a single isomer. The formation of **1** and **3** as the main products suggests that polymetallic rather than monometallic species may be the prevalent species in this yttrium *tert*-butoxide system. Indeed, complexes **3** and **1** may be the yttrium *tert*-butoxide equivalents of $(C_5H_5)_3Y(THF)$ and $(C_5H_5)_2YCl(THF)$, respectively. Complex **1** has one more Cl than **3**, as in their cyclopentadienyl analogues and **1** is formed by using 2 equiv of the ligand reagent, reaction 1, instead of 3 equiv, reaction 3, just as in the parallel cyclopentadienyl reactions 8 and 7. Parallels are also seen in reactivity studies (see below).

Equations 1–4 also show the importance of the alkali-metal cation of the alkoxide reagent. If high-yield syntheses of a single soluble product are desired, sodium is obviously preferred over lithium. This presumably is related to the tendency of lithium to be incorporated into the alkoxide product as in **4**. Lithium inclusion increases the number of structural variations, leading to mixtures of products, and can facilitate the formation of oligomerized low-solubility products.

Structure. The structure of complex **1** is an important variation of the trimetallic $Y_3(\mu_3\text{-OR})(\mu_3\text{-X})(\mu\text{-OR})_3$ framework (X = Cl, O, OR), which appears to be a basic structural unit in yttrium *tert*-butoxide chemistry.[30] The structure of **1** is very similar to that of **3**, even to the extent that distortions due to steric crowding can be observed. Taken together, the structures of **1** and **3** suggest that a variety of substituted versions of this trimetallic framework should be possible. As described previously,[30] trimetallic frameworks have been known for some time in metal alkoxide chemistry.[29,39–44] Structures such as $U_3(OCMe_3)_{10}O$[43] and $Mo_3[(OCH_2CMe_3)]_{10}O$[44] are two among many examples that have structural similarities to **1** and **3**. Hence, the trimetallic framework found in **1** and **3** is basic to many systems including those with tetravalent metals and metal–metal bonding.

The structure of **2** also provides examples of the $Y_3(\mu_3\text{-OR})(\mu_3\text{-X})(\mu\text{-OR})_3$ framework. More importantly, this structure and the fact that it can be obtained directly from **1** shows how easily changes in the basic $Y_3(\mu_3\text{-OR})(\mu_3\text{-X})(\mu\text{-OR})_3$ unit can be made to generate new variations. Unit A of **2** shows how a $Y_3(OR)_7Cl_2(THF)_2$ molecule can readily bridge via the chloride ligands to form oligomers. The existence of the tetrametallic portion of **2**, i.e., Y(1)–Y(4), suggests that the formation of tetrametallic **4** is not just a random event, but instead may be part of a general condensation reaction of $Y_3(OR)_7X_2$ molecules (R = CMe_3; X = OR, Cl). The Y(4)–$(\mu$-Cl$)_2$–Y(4a) portion of **2** is reminiscent of the interior of a $[(C_5H_5)_2Y(\mu\text{-Cl})]_2$ complex[45,46] in which oxide and alkoxide ligands replace the C_5H_5 groups. Hence, complex **2** combines structural features of several types of yttrium complexes and shows how they can be easily generated and linked together.

Trimetallic Reactivity. As shown in Scheme III, the dichloride complex **1** can be cleanly converted to the monochloride **3** by adding 1 equiv of NaOR (eq 9), but the attempted replacement of the chloride ion in **3** leads to insoluble products (eq 10). As discussed previously,[30] it is possible that a $Y_3(OR)_9(THF)_2$ structure in which a μ_3-OR has replaced the μ_3-Cl ligand in **3** may be too sterically crowded to exist. Note that with the larger metal lanthanum, the $La_3(OCMe_3)_9(THF)_2$ structure is accessible.[30] Hence, $Y_3(OR)_8Cl(THF)_2$ may be equivalent to the "peralkoxide" of this specific class of complexes, namely soluble neutral trimetallic yttrium *tert*-butoxides. The fact that a chloride ion in **1** is readily replaced suggests that this complex may be a good starting material for the synthesis of derivatives of these trimetallic species. Hence, in terms of reactivity as well as synthesis (see

(35) Masdiyasni, K. S.; Lynch, C. T.; Smith, J. S. *Inorg. Chem.* **1966**, *5*, 342–346. A more extensive list of lanthanide alkoxide references is given in ref 30.
(36) By using a much bulkier alkoxide ligand, 2,6-di-*tert*-butylphenoxide, a monomeric $Y(OR)_3$ structure has recently been obtained: Hitchcock, P. B.; Lappert, M. F.; Smith, R. G. *Inorg. Chim. Acta* **1987**, *139*, 183–184.
(37) Birmingham, J. M.; Wilkinson, G. *J. Am. Chem. Soc.* **1956**, *78*, 42–44.
(38) Maginn, R. E.; Manastyrskyj, S.; Dubeck, M. *J. Am. Chem. Soc.* **1963**, *85*, 672–676.
(39) Chisholm, M. H. *Polyhedron* **1983**, *2*, 681–721 and references therein.
(40) Cotton, F. A.; Extine, M. W.; Falvello, L. R.; Lewis, D. B.; Lewis, G. E.; Murillo, C. A.; Schwotzer, W.; Tomas, M.; Troup, J. M. *Inorg. Chem.* **1986**, *25*, 3505–3512.
(41) Dori, Z.; Cotton, F. A.; Llusar, R.; Schwotzer, W. *Polyhedron* **1986**, *5*, 907–909 and references therein.
(42) Coucouvanis, D.; Lester, R. K.; Kanatzidis, M. G.; Kessissoglou, D. P. *J. Am. Chem. Soc.* **1985**, *107*, 8279–8280.
(43) Cotton, F. A.; Marler, D. O.; Schwotzer, W. *Inorg. Chim. Acta* **1984**, *95*, 201–209.
(44) Chisholm, M. H.; Folting, K.; Huffman, J. C.; Kirkpatrick, C. C. *J. Am. Chem. Soc.* **1981**, *103*, 5967–5968.
(45) Atwood, J. L.; Smith, K. D. *J. Chem. Soc., Dalton Trans.* **1973**, 2487–2490.
(46) Baker, E. C.; Brown, L. D.; Raymond, K. N. *Inorg. Chem.* **1975**, *14*, 1376–1379.

synthesis section) **1** and **3** may be the trimetallic yttrium *tert*-butoxide analogues of the yttrium cyclopentadienyl complexes $(C_5H_5)_2YCl(THF)$ and $(C_5H_5)_3Y(THF)$, respectively.

Scheme III. Reactions of Trimetallic Yttrium *tert*-Butoxide Complexes (R = CMe_3)

$$\underset{\mathbf{1}}{Y_3(OR)_7Cl_2(THF)_2} + NaOR \rightarrow \underset{\mathbf{3}}{Y_3(OR)_8Cl(THF)_2} \quad (9)$$

$$\underset{\mathbf{3}}{Y_3(OR)_8Cl(THF)_2} + NaOR \rightarrow \text{insoluble products} \quad (10)$$

$$5\underset{\mathbf{1}}{Y_3(OR)_7Cl_2(THF)_2} \rightarrow \underset{\mathbf{2}}{Y_{14}(OR)_{28}Cl_{10}O_2(THF)_4} + 6THF + "Y_3^+" + 5RO^- + 2R^{+"} \quad (11)$$

Equations 9 and 10 provide the first data on the reactivity of these trimetallic species. The first point to be discussed is the stereoselectivity in eq 9. Two of the possible isomeric forms of $Y_3(OR)_8Cl(THF)_2$ are known: one that has both THF ligands on the μ_3-Cl side of the Y_3 plane, **3**, and one that has both THF ligands on the μ_3-OR side of the plane, **3'**. Complex **3**, the kinetically favored isomer, which is isolated exclusively from reaction 1, can be isomerized to **3'** in the presence of *tert*-butanol. When **1** reacts with NaOR (eq 9), it forms **3** almost exclusively. This stereoselectivity is reasonable considering that **1**, like **3**, has both THF ligands on the μ_3-Cl side of the Y_3 plane. This result suggests that substitution of this chloride can occur without major structural rearrangement.

Equations 9 and 10 also provide data on the relative reactivity of various ligand positions in this trimetallic system. Apparently, the terminal chloride ligand is more reactive than the triply bridging chloride ion in this reaction. This reactivity pattern is consistent with that observed previously for alkyl and hydride organoyttrium complexes, namely that terminal ligands are more reactive than doubly bridging ligands, which are more reactive than triply bridging ligands.[47-49]

It is possible that the triply bridging chloride ligand really is more reactive, and a subsequent rearrangement converts the unreacted terminal chloride ligand into the μ_3-Cl observed in the product. However, this seems unlikely since **3** is formed almost exclusively in eq 9 with only a trace amount of the isomer **3'** being found and since insoluble products result when the μ_3-Cl in **3** does react (eq 10). It is also possible that some prior activation reaction favors the terminal chloride ligand in this system and that its reactivity is not much different from that of the μ_3-Cl. However, the most likely reaction of this type is the dissociation of the THF ligands. Since these are adjacent to the μ_3 position and not to the terminal chloride, this is likely to favor the μ_3-Cl ion. Hence, eq 9 and 10 appear to establish the higher reactivity of the terminal chloride ligand in this system, at least with reagents the size of *tert*-butoxide.

Trimetallic to Polymetallic Reactivity. Complex **1** participates in a reaction even simpler than that in eq 9 when it is put in toluene, but the result is a much more complicated product. The conversion of **1** to **2** is described in eq 11 in a way that shows a possible theoretical stoichiometry. This reaction is remarkable in several ways. In terms of complexity, the self-assembly of the Y_{14} unit is the most complicated we have encountered so far. Yet the yield is quantitative. The stoichiometry in eq 11 shows that essentially *all* of the chloride ligands are incorporated into the product. It will be interesting to see how general this result is. The formation of oxide ligands, presumably from the alkoxide groups, under such mild reaction conditions is also surprising. We have observed several examples in which oxide ligands are formed in yttrium alkoxide reactions, so this apparently is a characteristic reaction option in these molecular systems. In all of the other systems, more complicated reactions occurred that formed multiple products. Equation 11 represents the cleanest and simplest oxide forming reaction observed to date for these yttrium alkoxides.

Part of the conversion of **1** to **2** can be readily visualized. It is possible that THF dissociates from **1** in toluene according to the equilibrium shown in eq 12. It is quite reasonable that a lone

$$Y_3(OR)_7Cl_2(THF)_2 \rightleftharpoons Y_3(OR)_7Cl_2(THF) + THF \quad (12)$$

pair on a terminal chloride ligand of a molecule of **1** could fill in the coordination position vacated by THF dissociation to form a $[Y_3(OR)_7Cl(THF)_2](\mu\text{-Cl})[Y_3(OR)_7Cl_2(THF)]$ unit (**6**). This corresponds to the A part of **2** linked to a trimetallic unit as it is in complex **2**. Further support of this process comes from the fact that **2** dissociates in THF to form some **1**.

Further analysis of the **1** to **2** conversion must be more speculative. Dissociation of THF from **1** and replacement with a $[Y_3(OR)_7Cl(THF)_2](\mu\text{-Cl})$ unit to form **6** as described above does not give the ligand arrangement found in **B**. The A–(μ-Cl)–B connection in **2** occurs at an yttrium atom, Y(2), that is attached to another chloride ligand, Cl(3). The connection between the trimetallic units in **6** occurs at an yttrium atom that is attached to a terminal alkoxide ligand. Hence, conversion of **6** to the A–B parts of **2** requires some ligand rearrangement in addition to the reaction that forms the oxide ligand. Examination of models suggests that there will be steric congestion in **6** which could lead to a rearrangement of ligands. However, more data must be collected on these systems before specific possible rearrangements can be evaluated.

Conclusions

The synthesis of **1** in high yield reinforces previous ideas on the prevalence of $Y_3(\mu_3\text{-OR})(\mu_3\text{-Cl})(\mu\text{-OR})_3$ units in yttrium *tert*-butoxide systems. The synthetic stoichiometries, the formulas, and the reactivities of **1** and **3** all suggest that these may be the yttrium *tert*-butoxide analogues of the cyclopentadienyl species $(C_5H_5)_2YCl(THF)$ and $(C_5H_5)_3Y(THF)$, respectively. In this regard, **1** will be an important starting material in this area.

The conversion of **1** to **2** provides the first well-defined example of how a molecular yttrium complex begins to form an extended polymetallic array. This example demonstrates that such transformations including oxide ligand formation can be studied at a molecular level. This also indicates that considerable rearrangement and a variety of structural permutations are possible under mild conditions. This suggests that the synthesis of solid-state yttrium oxide materials from yttrium alkoxides can be accomplished under mild conditions. Designed syntheses of specific materials will require close control of reaction conditions and a careful selection of precursor materials.

Experimental Section

All of the complexes described above are air- and moisture-sensitive. Therefore, both the syntheses and subsequent manipulations of these compounds were conducted with rigorous exclusion of air and water by using Schlenk, vacuum-line, and glovebox (Vacuum/Atmospheres HE-553 Dri-Lab) techniques. *tert*-Butyl alcohol was dried over and distilled from CaH_2. $NaOCMe_3$ was prepared from sodium in *tert*-butyl alcohol at 25 °C. Removal of the excess *tert*-butyl alcohol by rotary evaporation at 60–80 °C left a partially solvated material $NaOCMe_3 \cdot x Me_3COH$, x = 0.33–0.50 (by elemental analysis). Sublimation at 150 °C and 10^{-4} Torr gave the completely desolvated $NaOCMe_3$. Physical measurements and purification of the other reagents have been described previously.[30,45]

$Y_3(\mu_3\text{-OCMe}_3)(\mu_3\text{-Cl})(\mu\text{-OCMe}_3)_3(OCMe_3)_3Cl(THF)_2$ (1). In the glovebox, $NaOCMe_3$ (135 mg, 1.4 mmol) was dissolved in 6 mL of THF and added to a stirred suspension of YCl_3 (137 mg, 0.70 mmol) in 10 mL of THF. The solution was stirred overnight and centrifuged to remove an insoluble residue (which contained 8.6% yttrium). The remaining solution was evaporated to dryness, leaving a slightly oily solid. The solid was taken up in a minimum amount of toluene, and the resulting solution was centrifuged to remove some insolubles and evaporated to dryness, leaving **1** (172 mg, 74%). X-ray quality crystals of **1** were grown from a concentrated solution in THF at −34 °C. Anal. Calcd for $Y_3C_{36}H_{79}O_9Cl_2$: Y, 26.84. Found: Y, 26.0. Attempts to obtain complete elemental analyses were unsuccessful. Some representative results are given in the supplementary material. NMR data are given in Table I. IR (KBr): 2960 vs br, 1465 w, 1375 m, 1355 s, 1200 vs br, 1000 vs, 920 s, 865 m, 760 w, 740 vw cm^{-1}.

$[Y_7(\mu_3\text{-OCMe}_3)_2(\mu_3\text{-Cl})(\mu_4\text{-O})(\mu\text{-OCMe}_3)_7(OCMe_3)_5(\mu\text{-Cl})_4(THF)_2]_2$ (2). In the glovebox, **1** (170 mg, 0.17 mmol) was dissolved in 6 mL of

(47) Evans, W. J.; Dominguez, R.; Hanusa, T. P. *Organometallics* **1986**, *5*, 263–270.
(48) Evans, W. J. *Polyhedron* **1987**, *6*, 803–835.
(49) Evans, W. J. *Adv. Organomet. Chem.* **1985**, *24*, 131–177.

toluene and allowed to sit undisturbed at 29 °C for a period of 2 weeks. The solution was then centrifuged, removing a small amount of insoluble material. The remaining solution was evaporated to dryness, leaving **2** (150 mg, quantitative). X-ray quality crystals of **2** were grown from a concentrated solution in toluene at 29 °C. Anal. Calcd for $Y_{14}C_{128}H_{284}O_{34}Cl_{10}$: Y, 31.38. Found: Y, 31.1. NMR data are given in Table I. IR (KBr): 2960 vs br, 1460 w, 1380 sh, 1360 m, 1200 vs br, 1000 vs, 925 s, 870 w, 760 w cm^{-1}.

Synthesis of $Y_3(\mu_3\text{-OCMe})(\mu_3\text{-Cl})(\mu\text{-OCMe}_3)_3(OCMe_3)_4(THF)_2$ (3) from 1. In the glovebox, $NaOCMe_3$ (6 mg, 0.062 mmol) was dissolved in 3 mL of THF and added to a THF solution (8 mL) of **1** (61.3 mg, 0.062 mmol). After the mixture was stirred for approximately 10 min, a precipitate was visible in the solution. The mixture was allowed to stir overnight, after which time the solids were removed from the solution by centrifuging. The solution was then evaporated to dryness, leaving a somewhat oily residue. The residue was taken up in hexane and the resulting solution centrifuged to remove a small amount of insoluble material. The solution was evaporated to dryness, leaving **3** (50 mg, 80%), which was identified by ^1H NMR spectroscopy in Table I.

X-ray Crystallography of $Y_3(\mu_3\text{-OCMe}_3)(\mu_3\text{-Cl})(\mu\text{-OCMe}_3)_3(OCMe_3)_3Cl(THF)_2\cdot 2THF$. General procedures for data collection and reduction have been described previously.[50,51] An irregularly shaped crystal measuring 0.50 × 0.45 × 0.20 mm was selected for study. As soon as the crystal was removed from the mother liquor it began to desolvate, visually changing from clear to opaque. It was sealed under N_2 in a glass capillary and mounted on a Nicolet R3m/V diffractometer. Lattice parameters were determined at 25 °C from the angular settings of 25 computer-centered reflections with $21° < 2\theta < 27°$. Relevant crystal and data collection parameters for the present study are given in Table II. During the data collection, the intensities of three standard reflections, measured every 100 reflections, decreased by 46%; a linear correction for decay was later applied. The data were corrected for absorption.[51] Systematic absences established the space group as $P2_1/c$. The space group selection was supported at all stages of the structure solution and refinement. Direct methods (MITHRIL)[52] were used to locate the metal atoms, and difference Fourier techniques provided the positions of the remaining non-hydrogen atoms. All atoms with the exception of the *tert*-butyl carbons were refined with anisotropic thermal parameters by using full-matrix least-squares methods. Hydrogen atoms were not located. A final difference map revealed the presence of two disordered five-membered rings located at distances of 4.05 and 4.30 Å away from the nearest atom C(28). It is probable that these atoms represent what is left of two THF molecules of solvation. The exceptionally high decay of the crystal during data collection was most likely due to the loss of THF from the crystal lattice. This also explains why the crystals visibly changed when removed from solution and mounted. Some minor disorder was apparent in the *tert*-butyl groups. The final difference map contained residual electron density due to the disorder in these groups with no other recognizable features. Selected bond length data are given in Table III. Final fractional coordinates and complete bond length and angle data are given in the supplementary material.

X-ray Crystallography of $[Y_7(\mu_3\text{-OCMe}_3)_2(\mu_3\text{-Cl})(\mu_4\text{-O})(\mu\text{-OCMe}_3)_7(OCMe_3)_5(\mu\text{-Cl})_4(THF)_2]_2\cdot 2C_7H_8$. A crystal measuring 0.50 × 0.35 × 0.20 mm was sealed, along with some mother liquor, under N_2 in a glass capillary and was handled as described above for **1**. Lattice parameters were determined at 25 °C from the angular settings of 15 computer-centered reflections with $4° < 2\theta < 22°$. Relevant crystal and data collection parameters for the present study are given in Table II. During the data collection, the intensities of three standard reflections measured every 100 reflections remained constant. The data were corrected for absorption.[51] The space group was determined for lack of any systematic absences, to be $P1$ or $P\bar{1}$. Statistics favored the centrosymmetric $P\bar{1}$. This choice was fully supported at all stages of the structure refinement and solution. Direct methods (MITHRIL)[52] were used to locate the metal atoms, and difference Fourier techniques provided the positions of the remaining non-hydrogen atoms. All atoms with the exception of the *tert*-butyl carbons and O(2), O(3), O(6), and O(7) were refined with anisotropic thermal parameters by using full-matrix least-squares methods. One of the 14 *tert*-butyl groups, the one designated by C(12), C(48), C(49), and C(50) failed to refine in a satisfactory manner. Consequently, the positions of the atoms associated with this group were determined from a difference map and fixed during subsequent refinement. Hydrogen atoms were not located. A final difference map revealed the presence of two disordered six-membered rings located at distances of 3.63 and 3.49 Å away from the nearest atoms, C(12) and C(52), respectively. The NMR data are consistent with these being toluene molecules. The final difference map contained no other recognizable features. Selected bond length data are given in Table III. Final fractional coordinates and complete bond length and angle data are given in the supplementary material.

Acknowledgment. For support of this research, we thank the Division of Chemical Sciences of the Office of Basic Energy Sciences of the Department of Energy. We thank Dr. Joseph W. Ziller for helpful discussion.

Supplementary Material Available: A listing of elemental analytical data and tables of complete crystallographic data, positional parameters, bond distances and angles, and thermal parameters (15 pages); tables of structure factor amplitudes (30 pages). Ordering information is given on any current masthead page.

(50) Sams, D. B.; Doedens, R. J. *Inorg. Chem.* **1979**, *18*, 153–156.
(51) Computations were carried out with a local version of the UCLA Crystallographic Computing Package (C. E. Strouse). Strouse, C. E., personal communication to R. J. Doedens. Graphics and empirical absorption were done with SHELXTL-Plus programs.
(52) Gilmore, C. J. "MITHRIL, A Computer Program for the Automatic Solution of Crystal Structures from X-ray Data", University of Glasgow.